IOP PUBLISHING CLASSICAL AND QUANTUM GRAVITY

Class. Quantum Grav. **24** (2007) S617–S625 doi:10.1088/0264-9381/24/19/S24

Improving the timing precision for inspiral signals found by interferometric gravitational wave detectors

F Acernese[1], P Amico[2], M Alshourbagy[3], F Antonucci[4], S Aoudia[5], P Astone[4], S Avino[1], D Babusci[6], G Ballardin[7], F Barone[1], L Barsotti[3], M Barsuglia[8], Th S Bauer[9], F Beauville[10], S Bigotta[3], S Birindelli[3], M A Bizouard[8], C Boccara[11], F Bondu[5], L Bosi[2], C Bradaschia[3], S Braccini[3], F J van den Brand[9], A Brillet[5], V Brisson[8], D Buskulic[10], E Calloni[1], E Campagna[12], F Carbognani[7], F Cavalier[8], R Cavalieri[7], G Cella[3], E Cesarini[12], E Chassande-Mottin[5], N Christensen[7], C Corda[3], A Corsi[4], F Cottone[2], A-C Clapson[8], F Cleva[5], J-P Coulon[5], E Cuoco[7], A Dari[2], V Dattilo[7], M Davier[8], M del Prete[3], R De Rosa[1], L Di Fiore[1], A Di Virgilio[3], B Dujardin[5], A Eleuteri[1], M Evans[7], I Ferrante[3], F Fidecaro[3], I Fiori[7], R Flaminio[7,10], J-D Fournier[5], S Frasca[4], F Frasconi[3], L Gammaitoni[2], F Garufi[1], E Genin[7], A Gennai[3], A Giazotto[3], G Giordano[6], L Giordano[1], R Gouaty[10], D Grosjean[10], G Guidi[12], S Hamdani[7], S Hebri[7], H Heitmann[5], P Hello[8], D Huet[7], S Karkar[10], S Kreckelbergh[8], P La Penna[7], M Laval[5], N Leroy[8], N Letendre[10], B Lopez[7], Lorenzini[12], V Loriette[11], G Losurdo[12], J-M Mackowski[5], E Majorana[4], C N Man[5], M Mantovani[3], F Marchesoni[2], F Marion[10], J Marque[7], F Martelli[12], A Masserot[10], M Mazzoni[12], L Milano[1], F Menzinger[7], C Moins[7], J Moreau[11], N Morgado[5], B Mours[10], F Nocera[7], C Palomba[4], F Paoletti[3,7], S Pardi[1], A Pasqualetti[7], R Passaquieti[3], D Passuello[3], F Piergiovanni[12], L Pinard[13], R Poggiani[3], M Punturo[2], P Puppo[4], S van der Putten[9], K Qipiani[1], P Rapagnani[4], V Reita[11], A Remillieux[13], F Ricci[4], I Ricciardi[1], P Ruggi[7], G Russo[1], S Solimeno[1], A Spallicci[5], M Tarallo[3], M Tonelli[3], A Toncelli[3], E Tournefier[10], F Travasso[2], C Tremola[3], G Vajente[3], D Verkindt[10], F Vetrano[12], A Viceré[12], J-Y Vinet[5], H Vocca[2] and M Yvert[10]

[1] INFN, sezione di Napoli and/or Università di Napoli 'Federico II' Complesso Universitario di Monte S.Angelo, and/or Università di Salerno, Fisciano (Sa), Italy
[2] INFN, Sezione di Perugia and/or Università di Perugia, Perugia, Italy
[3] INFN, Sezione di Pisa and/or Università di Pisa, Pisa, Italy
[4] INFN, Sezione di Roma and/or Università 'La Sapienza', Roma, Italy
[5] Departement Artemis, Observatoire de la Côte d'Azur, BP 42209 06304 Nice, Cedex 4, France
[6] INFN, Laboratori Nazionali di Frascati, Frascati (Rm), Italy
[7] European Gravitational Observatory (EGO), Cascina (Pi), Italy
[8] LAL, Univ Paris-Sud, IN2P3/CNRS, Orsay, France
[9] NIKHEF, NL-1009 DB Amsterdam and/or Vrije Universiteit, NL-1081 HV Amsterdam, The Netherlands
[10] Laboratoire d'Annecy-le-Vieux de Physique des Particules (LAPP), IN2P3/CNRS, Université de Savoie, Annecy-le-Vieux, France
[11] ESPCI, Paris, France
[12] INFN, Sezione di Firenze/Urbino, Sesto Fiorentino, and/or Università di Firenze, and/or Università di Urbino, Italy
[13] LMA, Villeurbanne, Lyon, France

0264-9381/07/190617+09$30.00 © 2007 IOP Publishing Ltd Printed in the UK

Received 6 May 2007, in final form 27 August 2007
Published 19 September 2007
Online at stacks.iop.org/CQG/24/S617

Abstract
As they take data and improve their sensitivities, interferometric gravitational wave detectors will eventually detect signals emitted by inspiralling compact binary systems. Determining the sky position of the source will require that the signal be recorded in several detectors. The precision of the source direction determination will be driven by that of the time-of-flight measurements between detectors, and ultimately by the timing precision at the level of each detector. The latter is limited by the noise of the detector and the use of template banks, which introduce some mismatches between the parameters of the signal and the parameters of the template used to detect it. The standard way for signal timing is based on referring to the end time of the signal. In this paper we show that this is not an optimal choice and the timing precision can be improved referring to a time when the signal crosses some reference frequency, whose optimal value depends on the detector sensitivity.

PACS numbers: 04.80.Nn, 95.55.Ym, 07.05.Kf

(Some figures in this article are in colour only in the electronic version)

Introduction

Around the world, several interferometric gravitational wave detectors are now being operated and are taking data at or close to their design sensitivities. Further upgrades to improve the sensitivity of those detectors are planned. Eventually a time will come when this network of detectors will be able to record gravitational wave signals coincidently in several detectors.

Among the classes of potential signals, we consider in this paper the signals emitted through the last stages of the inspiralling phase of compact binary systems. Those signals are expected to appear as chirps sweeping through the frequency bandwidth of the detectors. The possibility of modeling accurately the waveform emitted by a source of known parameters allows us to use matched filtering to search for such signals. As the source parameters are not known *a priori*, waveform families—called template banks—are used to sample the parameter space.

Estimating the sky position of a source usually requires detecting the signal in at least three differently located detectors, and involves measuring the signal time of flight between the detectors. Such a measurement is limited by the precision with which the time of arrival of the signal at each detector can be determined. The uncertainties in this measurement arise from the mismatch between the parameters of the signal and the triggering template, which causes the template and true signal not to overlap perfectly and results in some timing errors. This will happen even if the template bank provides a very fine sampling of the parameter space, as detector noise will cause random excursions across the template bank.

The time which is most straightforwardly extracted from a matched filtering procedure is the arrival time of the signal, namely the time when the signal crosses some minimum frequency $f_{\min}$ corresponding to the detector bandwidth lower frequency. It is well known however [1] that the arrival time is very sensitive to parameter mismatch between signal and template, and the precision can be improved considering the signal end time, i.e. the time

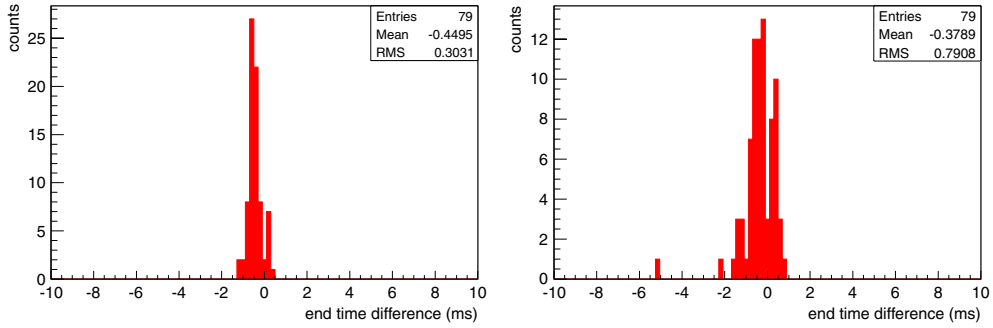

Figure 1. Timing resolution obtained on simulated Virgo data, using the signal end time, as the difference between the estimated and true values. Left: with an exact template. Right: with a template bank. Both distributions exhibit a small but statistically significant bias. No attempt has been made to correct this bias as it is approximately the same in all detectors and vanishes when the time differences—which are the relevant quantities—are taken.

when the signal reaches its maximum frequency $f_{\max}$. In practice, the end time is obtained by extracting the arrival time from the matched filtering procedure, and adding the duration of the triggering template. In this paper we show that the timing precision can be further improved by considering the time when the signal crosses some reference frequency lying somewhere between $f_{\min}$ and $f_{\max}$. To do so, we use simulated data featuring the LIGO–Virgo network and including astrophysical inspiral signals. Those data were generated in the framework of the joint LIGO–Virgo working group in preparing for joint searches [2].

This paper is organized as follows. In section 1 we focus on the timing precision at the level of individual detectors, introduce the reference time and compare the accuracies which can be obtained with various methods. In section 2 we extend the results of section 1 to the time of flight of a signal between detectors. Finally in section 3 we apply the results of section 2 to better estimate the sky position of the source of a signal.

1. Single detector timing precision and reference time

In this section we consider the timing precision at the level of the individual detectors in the LIGO–Virgo network. We use simulated data produced to prepare joint LIGO–Virgo searches. They consist of 24 h of data with noise at the design sensitivities of the instruments, and 145 2.0 post-Newtonian inspiral signals (called injections) generated with individual star masses uniformly distributed between the values 1, 1.4, 2 and 3 solar masses, thus roughly sampling the neutron star mass parameter space, and originating from two galaxies at 16 and 10 Mpc.

Matched filter searches were performed on those data, and in the following we consider injections detected with a signal-to-noise ratio (SNR) of at least 6, which is the case of about one half of the injections.

1.1. Timing precision with end time

We review here the results obtained using the signal end time to measure the time of the detected injections. In figure 1 we compare the timing resolution for injections detected in the Virgo data in two different cases: the left plot was obtained by performing a matched filter analysis with exact templates (i.e., with masses equal to the injection parameters) while the

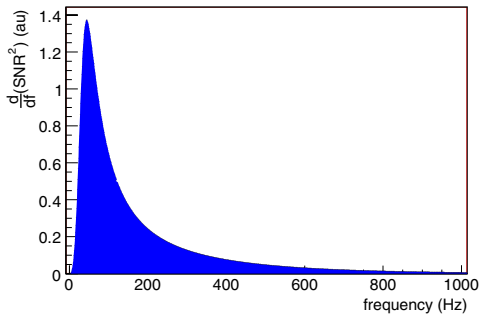

Figure 2. Density of squared SNR as a function of frequency for a [1.4–1.4] $M_\odot$ inspiral signal in the Virgo detector at design sensitivity.

right plot was obtained by performing a matched filter analysis with a template bank generated over the [1–3] $M_\odot$ mass range with a minimal match of 95%.

In the exact template case, the resolution is limited by the statistical fluctuations due to the noise, and by the fact that the data are processed as discrete time series sampled with a finite frequency, here 4 kHz. (No attempt was made here to interpolate the SNR time series to improve the determination of the maximum position in time.) In the template bank case the resolution is worse by about a factor of 3 and is limited by the parameter mismatch between the signal and the template which detected the injection.

Neither of these resolutions are absolute results. They both depend on the SNR of the events and in the second case depend on the density of the template bank, driven by the minimal match used. They nevertheless serve our purpose which is to recall how timing resolution is affected by parameter uncertainties inherent to a search based on a template bank. In the next section we discuss how this effect can be mitigated.

1.2. Timing precision with reference time

The reason why detecting a signal with a mismatched template results in some timing error is that the phase evolution and the time it takes to sweep through the detector bandwidth are different for the template and the true signal. The maximization involved in the matched filtering procedure finds how the template should be shifted with respect to the true signal to get the best overlap between the two signals, quantified in terms of SNR. However the SNR does not accumulate uniformly across the detector bandwidth (see figure 2) and therefore the matched filtering selects a particular template and a particular arrival time to best overlap the signal in some frequency range which matters for the SNR. On the other end, the phase difference resulting in a timing error accumulates across the full frequency band. Hence the idea that referring the timing to some reference frequency in the high SNR density region could improve the resolution. This is illustrated in figure 3.

We therefore introduce a reference time t_{ref,f_S} at some reference frequency f_S defined as

$$t_{\mathrm{ref},f_S} = t_0 + T_{f_0 \to f_S}, \tag{1}$$

where t_0 is the time when the signal crosses the analysis minimum frequency f_0, measured as the time when the correlation between the data stream and the best-matching template reaches a maximum, and $T_{f_0 \to f_S}$ is the time it takes for an inspiral signal with the template parameters to sweep from the frequency f_0 to the reference frequency f_S. With this notation, the standard end time can be rewritten as $t_{\mathrm{ref},f_{\mathrm{max}}}$ with f_{max} being the signal maximum frequency.

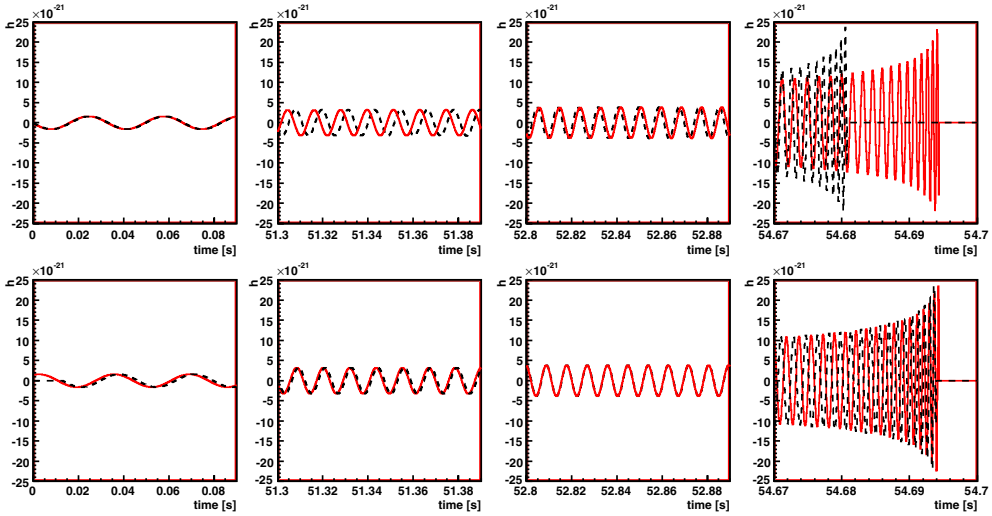

Figure 3. This figure illustrates what happens in the matched filtering maximization process that makes the reference time a better estimator for signal timing. It is derived from a concrete example taken from the simulation that was performed for this study, where a [1.4, 1.4]$M_{\odot}$ injection was detected by a [1.153, 1.712]$M_{\odot}$ template in the Virgo data. The two signals—true waveform as dashed line and mismatched template as solid line—are drawn showing from left to right snapshots at 30 Hz, 100 Hz, 170 Hz and at the end of the signal. On the top figures, the signals are drawn both starting at the same time and phase at the initial frequency of 30 Hz. This illustrates simply how the phase evolution differs for the two signals, and especially the fact that the duration of the mismatched template is significantly different from the duration of the true waveform. The optimization involved in the matched filtering procedure however allows for some time and phase offsets between the template and the true signal when maximizing the SNR. In other words, the template is translated and rotated in a way that leads to the best match with the true signal in terms of SNR, i.e. in the frequency band where the detector sensitivity is the best. The result of this optimization is shown in the bottom figures where a time delay and a phase offset have been applied to the mismatched template—using the actual values coming out of the analysis. The snapshot at 30 Hz shows that the arrival time for the template differs significantly from the true signal arrival time—this illustrates the well-known result that the arrival time is a poor estimator for signal timing. The snapshot at the end of the signal illustrates that the end time is a better estimator than the arrival time, but still differs from the true end time by about 0.4 ms in this case. The snapshots around 100 Hz and 170 Hz show that at these frequencies the phase evolution of the template matches that of the signal quite well, explaining why timing the signal at a reference frequency in this region would give a better result. Again the fact that the template follows closely the true signal in the intermediate frequency region does not happen by chance but because this is where the detector is the most sensitive, therefore 'aligning' the two signals here would lead to the best SNR.

We then investigate the quality of t_{ref,f_S} as a timing estimator as a function of the reference frequency f_S. For each value of f_S, we build the distribution of the error in t_{ref,f_S} (as the difference between the value reported by the template and the true signal value) and extract the standard deviation of this distribution, which we plot against f_S in figure 4, for the injections detected in each of the H1, L1 and Virgo detectors. The error on each point is computed as the distribution standard deviation divided by $\sqrt{2(N-1)}$ where N is the number of injections entering the distribution.

The dependence of the reference time precision with f_S is such that for large values of f_S it tends as expected toward the precision obtained with the end time, and exhibits a broad minimum around a frequency of 160 Hz, where it comes close to the value obtained with the

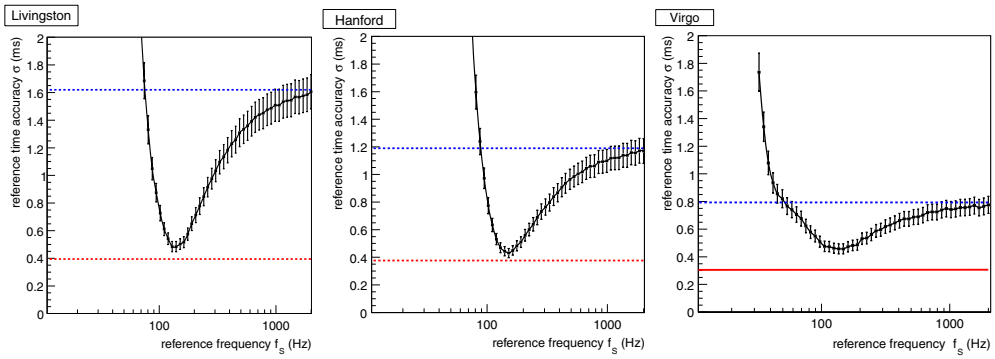

Figure 4. Evolution of the precision obtained with the reference time as a function of the reference frequency f_S, for the injections detected in each of the L1, H1 and Virgo detectors. The dashed line indicates the precision obtained with a template bank and the end time. The solid line indicates the precision obtained with exact templates. The error bars on those lines are not shown as they are correlated to the error bars on the points.

Table 1. This table lists the optimal precision $\sigma_{\rm opt}$ obtained using the reference time at the optimal f_S frequency. The optimal precision is compared to the precision $\sigma_{\rm std}$ obtained with the end time and a template bank built with a minimal match of 95% and to the precision $\sigma_{\rm exact}$ obtained using exact templates. Since the resolution depends on the SNR of the events, the average and maximum values of the SNR for the detected injections are listed for each detector.

Detector	L1	H1	Virgo
Mean (max) SNR of detected injections	10.9 (26.7)	10.7 (28.5)	7.3 (20.8)
Optimal f_S (Hz)	155 ± 20	160 ± 20	170 ± 40
$\sigma_{\rm exact}$ (ms)	0.39 ± 0.03	0.38 ± 0.03	0.30 ± 0.02
$\sigma_{\rm opt}$ (ms)	0.47 ± 0.04	0.43 ± 0.03	0.48 ± 0.04
$\sigma_{\rm std}$ (ms)	1.61 ± 0.12	1.18 ± 0.09	0.79 ± 0.06

exact template analysis. This demonstrates that the timing uncertainties arising from the use of a finite density template bank to sample the signal parameter space can be mitigated using a reference time at a frequency where the SNR density is high.

These results are summarized in table 1. The improvement brought by the optimal reference time precision over the precision obtained with the end time is about a factor of 3 on LIGO data, and a factor of 1.6 on Virgo data. The optimal reference time precision approaches the precision obtained with exact templates within a factor of 1.2 on LIGO data and a factor of 1.6 on Virgo data.

In general we expect the optimal reference frequency to be mass dependent as the total mass of the binary system affects the frequency evolution of the signal. The frequency dependence of the reference time precision shows however a broad minimum; therefore using a fixed value for the reference frequency should result in a small loss of optimality for a fairly large range of masses. It would however be straightforward to use a mass-dependent reference frequency and this would probably be needed if searching for binaries with a total mass large enough to significantly shift the SNR density down to lower frequencies.

It should be noted that using the reference time reduces the correlation between the chirp mass error and the time error and therefore mitigates the effect of detecting a signal with a slightly mismatched template, but does not improve the precision on the chirp mass itself,

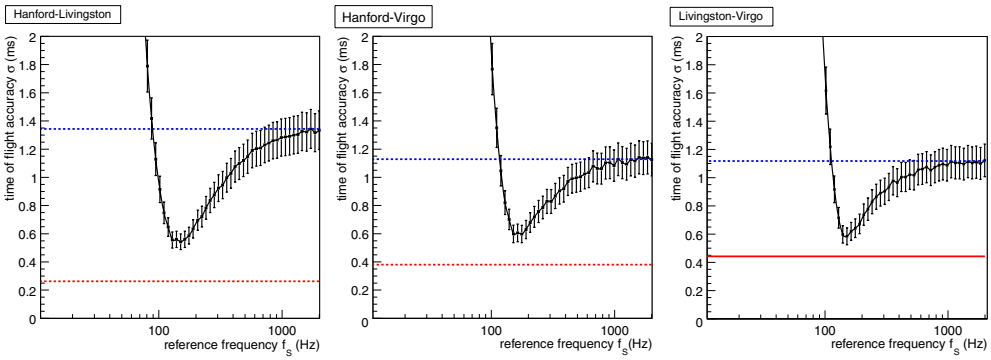

Figure 5. Evolution of the time-of-flight precision obtained with the reference time as a function of the reference frequency f_S, for the injections detected in all of the H1, L1 and Virgo detectors. The dashed line indicates the precision obtained with a template bank and the end time. The solid line indicates the precision obtained with exact templates. The error bars on those lines are not shown as they are correlated to the error bars on the points.

Table 2. This table lists the optimal time-of-flight precision $\sigma_{\rm opt}$ obtained using the reference time at the optimal f_S frequency. The optimal precision is compared to the precision $\sigma_{\rm std}$ obtained with the end time and a template bank built with a minimal match of 95% and to the precision $\sigma_{\rm exact}$ obtained using exact templates. Since the resolution depends on the SNR of the events, the average SNR value of the injections detected in coincidence is listed for each detector.

Detector	L1	H1	Virgo
Mean SNR of detected coincidences	12.1	12.6	11.6
Detector pair	H1-L1	H1-V	L1-V
Optimal f_S (Hz)	155 ± 20	180 ± 40	155 ± 40
$\sigma_{\rm exact}$ (ms)	0.26 ± 0.03	0.38 ± 0.04	0.44 ± 0.05
$\sigma_{\rm opt}$ (ms)	0.52 ± 0.04	0.50 ± 0.05	0.57 ± 0.06
$\sigma_{\rm std}$ (ms)	1.34 ± 0.14	1.12 ± 0.12	1.10 ± 0.11

which remains unchanged. A related comment is that in the case when the exact templates are used, using the reference time or the end time is equivalent.

2. Network time-of-flight precision

In this section we focus on the precision of the time of flights measured between detectors of the network. This follows quite straightforwardly from the results presented above. We now consider the simulated signals detected with coincident times in the three detectors (there are 47 such triple coincidences out of the 145 injections). For those, and for each detector pair, we compare the precision which can be obtained taking the difference between the reference times measured at the two detectors, as a function of f_S, to the accuracies which would be obtained using the end time or exact templates.

The f_S dependence of the time-of-flight precision is shown in figure 5, and the results are summarized in table 2. The reference time at the optimal f_S brings an improvement of about a factor of 2 in the time-of-flight accuracies with respect to the end time.

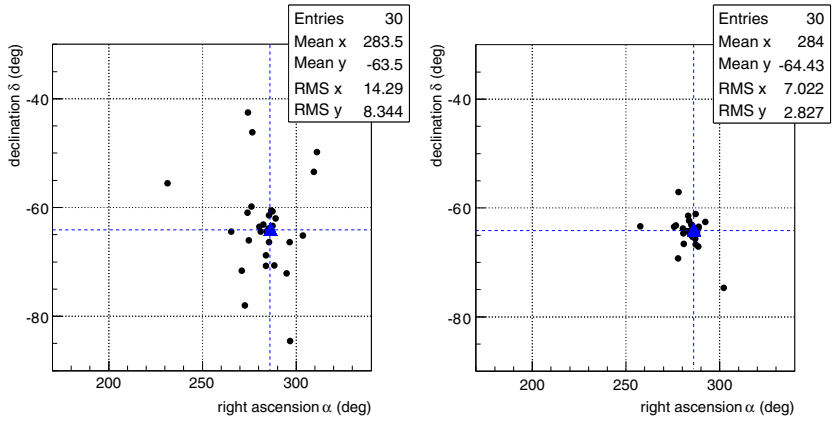

Figure 6. Estimated source direction for the injections simulated as originating from galaxy NGC 6744 (the triangle at the crossing of the dashed lines indicates the true source position). Left: direction estimated using the end time. Right: direction estimated using the reference time at $f_S = 160$ Hz.

3. Consequences on source direction estimation

In this section we show the improvement in the source direction reconstruction which can be derived from the improvement in the time-of-flight precision brought by the reference time. Obviously one needs to use the same reference frequency to measure the times of flight between all detector pairs. Since the optimal reference frequency depends on the sensitivity and is therefore different for Virgo and the LIGO detectors, a common value will inevitably be sub-optimal for some of the detectors. However the resolution shows a broad minimum around the best reference frequency and therefore one should be close to optimal using a common reference frequency of 160 Hz.

Here we consider, among the signals detected coincidently in the three detectors, the 30 injections which were simulated as originating from the galaxy NGC 6744 distant by 10 Mpc and located at a right ascension of 286° and a declination of 64°. For those injections, the source direction can be estimated—using a χ^2 minimization fit—from the time delays measured between the detectors. The minimized quantity is

$$\chi^2 = \frac{[\Delta t_{\mathrm{HL}} - \Delta t'_{\mathrm{HL}}(m_1, m_2, \alpha, \delta, t_0)]^2}{\sigma^2} + \frac{[\Delta t_{\mathrm{LV}} - \Delta t'_{\mathrm{LV}}(m_1, m_2, \alpha, \delta, t_0)]^2}{\sigma^2}, \tag{2}$$

where Δt_{HL} and Δt_{LV} are the measured time delays between the Hanford and Livingston detectors and between the Livingston and Virgo detectors (using either the end time or the reference time). The $\Delta t'$ are the expected time delays assuming the source has some mass parameters m_1 and m_2, a direction (α, δ) and the signal reaches the Earth at time t_0 (which does not need to be determined with great precision). The $\Delta t'$ are computed from the apparent longitude of a source located at (α, δ) at time t_0. The error parameter σ was set to a value of 1 ms. In this equation, Δt_{HL}, Δt_{LV} and t_0 come out of the analysis, as do m_1 and m_2 (taken as the parameters of the template giving the highest SNR). The only free parameters are α and δ which can be estimated by minimizing χ^2.

In figure 6 we compare the direction precision obtained from time delays based on the end time and the precision obtained from time delays based on the reference time at 160 Hz.

As expected, the improved timing resolution with the reference time directly translates into an improved precision for the source direction estimation.

4. Conclusion

In this paper we have shown how the timing of inspiral signals can be improved using, instead of the signal end time, a reference time at a frequency located in the region where the signal SNR density is high. The quantitative results depend on the particular parameters of the present study—especially through the SNR of the simulated events and the minimal match used to generate the template bank. We however believe that they are representative of the situation that a network of first generation interferometric gravitational wave detectors could face. We have also shown how one can take advantage of the improved timing precision to better reconstruct the source position for a signal found coincidentally in the detectors of the LIGO–Virgo network. We hope this is a simple way to approach the best direction reconstruction which can in principle be achieved with more sophisticated methods based on various flavors of coherent analysis [3, 4].

We expect it will be straightforward to implement the use of the reference time in actual analysis pipelines as the only change to the analysis is to introduce a delay in the definition of the signal time. As this delay depends only on the chosen reference frequency and the template mass parameters, this is a simple change to do.

In future work it would be interesting to check how the reference time behaves when one varies the model used to compute the waveforms and the injections are searched for with mismatched template families, which leads to further timing errors. Since signal models usually differ most at the end of the signal, one could hope that using the reference time would bring a significant improvement, but further study will be needed to investigate this.

References

[1] Balasubramanian R, Sathyaprakash B S and Dhurandhar S V 1996 *Phys. Rev.* D **53** 3033
[2] Beauville F *et al* (LIGO/Virgo working group) 2007 submitted to *Class. Quantum Grav.* (*Preprint* gr-qc/0701027)
[3] Pai A, Dhurandhar S and Bose S 2001 *Phys. Rev.* D **64** 042004
[4] Rover C, Meyer R and Christensen N 2007 *Phys. Rev.* D **75** 062004